

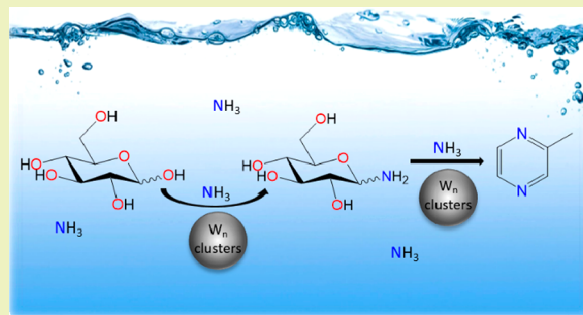
One-Step Synthesis of N-Heterocyclic Compounds from Carbohydrates over Tungsten-Based Catalysts

Xi Chen, Huiying Yang, Max J. Hülsey, and Ning Yan*[✉]

Department of Chemical and Biomolecular Engineering, National University of Singapore, Blk E5, 4 Engineering Drive 4, Singapore 117585, Singapore

Supporting Information

ABSTRACT: A one-step reaction system has been developed to convert glucose and other renewable carbohydrates into important N-heterocyclic compounds in ammonia solution. Under optimal conditions, 2-methyl pyrazine (MP) and 4(5)-methyl imidazole (MI) were produced within 15 min with combined yields of around 40%. While the formation of 4(5)-MI was identified as a noncatalytic process, the yield of 2-MP was highly influenced by the presence of catalysts. In particular, nearly 3-fold yield enhancement of 2-MP was achieved over several tungsten-based catalysts. Control experiments, isotope-labeling tests, ESI-MS, and NMR analysis revealed that the formation of 2-MP follows a fragmentation mechanism, while small tungsten clusters such as $[\text{HW}_2\text{O}_7]^-$ and $[\text{W}_4\text{O}_{13}]^{2-}$ were the catalytically active species facilitating both glucose fragmentation and the subsequent cyclization reaction to generate pyrazine rings. The work exemplifies the possibility of sustainable production of important N-containing, heterocyclic chemicals from woody biomass, where the identification and understanding of novel catalysts are the key.



KEYWORDS: Biomass, Sugar, Pyrazine, Ammonia, N-Containing compound, Sustainable catalysis, Isotope labeling, Reaction pathway

INTRODUCTION

There is a desire to obtain commodity chemicals and fine chemicals from renewable resources such as biomass, for the benefits of the environment and the sustainable development of society.^{1–7} Considerable efforts have been directed to the conversion of woody biomass into a variety of oxygen-functionalized chemicals via different chemical routes.^{8–19} Nevertheless, much less attention has been paid to other heteroatom-containing chemicals, such as those bearing nitrogen, sulfur, and phosphorus,^{20–22} despite their crucial roles in agricultural, pharmaceutical, food, and cosmetic applications. For instance, 2-methyl pyrazine (2-MP) is a core unit for the synthesis of the antitubercular drug pyrazinamide and bacteriostatic agents, while 4(5)-methyl imidazole (4(5)-MI) is an integral unit for drug Temozolomide to treat brain cancers. Unfortunately, current manufacturing of these N-heterocyclic compounds are not highly efficient. Taking the synthesis of 2-MP as an example, multiple chemical steps are required to first generate ethylenediamine and propylene glycol from petroleum, which are building blocks for subsequent cyclization and dehydration or dehydrogenation reactions to finally form the product.^{23–26} Therefore, it is highly advantageous to develop synthetic tools to produce N-heterocyclic chemicals such as pyrazines and imidazole from renewable biomass in a straightforward and more efficient way.

Synthesis of N-heterocyclic chemicals from biomass components is not unreported. In food chemistry, the formation of trace amounts of pyrazines between renewable

sugars and amino acids is a well-understood process, namely the Maillard reaction.²⁷ Reactions of carbohydrates in ammonia solution at room or elevated temperatures have also been investigated which led to the nonselective generation of a mixture of N-heterocyclic chemicals in relatively low yields.^{28,29} For example, the total yields of pyrazines were less than 1 wt % from glucose reaction in ammonium hydroxide at elevated temperature.³⁰ We have reported the formation of pyrrole with up to 6% carbon yield from chitin.³¹ During the preparation of this manuscript, a noncatalytic process was reported to obtain 2-hydroxymethyl-5-methylpyrazine with high yield from biomass-derived 1,3-dihydroxyacetone using diammonium phosphate as the nitrogen source in water/dioxane solvent.³² In general, however, there is still a lack of efficient transformation systems to produce N-heterocyclic compounds from biomass resources.

Ideally, the starting biomass resource provides both renewable carbon and nitrogen atoms (such as chitin), as proposed in the concept of shell biorefinery³³ and practiced in the synthesis of amino polyols,^{34,35} furans,^{36–41} organic acids,^{31,42,43} and others.⁴⁴ Nevertheless, the generation of N-heterocyclic compounds such as pyrazines from chitin is not practical, since the nitrogen to carbon ratio in the product (1:4–6) far exceeds that in the starting material (1:8).³¹ Glucose is the

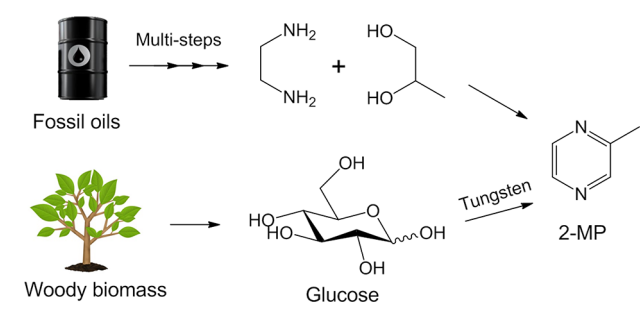
Received: August 31, 2017

Revised: October 10, 2017

Published: October 16, 2017

most abundant renewable sugar that can be easily obtained from inedible cellulosic biomass. In this paper, the objective is to achieve the one-step synthesis of N-heterocyclic products such as 2-MP from glucose and other carbohydrates via an effective catalytic system using aqueous ammonia as the nitrogen source, offering a competing synthetic route to the conventional method (see Scheme 1).

Scheme 1. Conventional Synthesis of 2-MP (Top) and the Proposed Tungsten-Assisted One-Step Conversion of Glucose to 2-MP (Bottom)



EXPERIMENTAL SECTION

Chemicals and Materials. Glucose and ammonia solution (25 wt %) were purchased from Merck. Cellobiose, tungsten oxide (WO_3), silicotungstic acid hydrate, and ammonium tungstate hydrate were from Sinopharm Chemical Reagent. Ammonium metatungstate, phosphotungstic acid, sodium tungstate dihydrate, the standards of pyrazine compounds (including pyrazine, 2-methyl pyrazine, 2,3-dimethyl pyrazine, 2,3,5-trimethyl pyrazine, etc.), glyceraldehyde, glycolaldehyde dimer, erythrose, xylose, fructose, sucrose, maltose, 5-HMF, glucosamine, inulin, ammonium formate (NH_4COOH), sodium chloride, ammonia in methanol (7 N), ammonium chloride (NH_4Cl), diammonium phosphate (DAP), and other chemicals were purchased from Sigma-Aldrich. Cellulose was from Alfa Aesar. ^{13}C -labeled glucose samples were from Omicron Biochemicals Inc.

General Procedures. In a typical reaction, 100 mg (0.55 mmol) of glucose was dissolved in 5 mL of 25 wt % ammonia solution with or without the addition of a certain amount of tungsten catalyst. The reaction mixture was loaded into a reactor with a valve. The reactor was sealed and put into a steel holder with insulating jacket heated by a hot plate. The thermal sensor was inserted into the steel holder, and the temperature was preset to the desired value prior to the reaction. After reaction, the reactor was taken out, cooled under flowing water, moved to a fume hood, and opened. Afterward, 50 μL of 1,4-dioxane (internal standard) was added, and the reaction solution was transferred into a volumetric flask and diluted to 10 mL. Then, 1 mL of the solution was taken and filtered by a PTFE membrane with a pore size of 0.45 μm and analyzed by gas chromatography-flame ionization detector (GC-FID Agilent 7890A GC with a flame ionization detector). A less concentrated ammonia solution was obtained by diluting the commercial 25% solution with water. A more concentrated ammonia solution (>25%) was prepared by constantly purging ammonia gas into the commercial ammonia solution in a reactor under high pressure.

Product Identification and Quantification. The product identification and quantification were mainly achieved by using GC-FID with a BP-5 capillary column. Authentic standards of pyrazine compounds were injected, and the retention time was compared. In addition, the major products were extracted by dichloromethane and examined on gas chromatography–mass spectroscopy (GC-MS, an Agilent 7890A GC system with 7693 Autosampler and S975C inert MSD with triple-axis detector) by using a HP-5 capillary column. The products were also examined by UPLC-ESI-MS (model 8030, Shimadzu) with an autosampler (CTC Analytics AG, Zwinger), LC-

30AD binary pumps, a DGU-20A degasser, and a CTO-30A column oven. A Luna C18 column (5 μm particle diameter, 150 mm \times 4.6 mm², Phenomenex) was used. HPLC analysis was run in isocratic mode with water:acetonitrile = 97:3, containing 0.1% formic acid in water. Sugar conversion was quantified over a Shimadzu Nexera XR HPLC system equipped with SPD-M30A and RID-20A detectors and an SIL-20AC autosampler. An Agilent Hi-Plex H column was used at 60 $^\circ\text{C}$ with the mobile phase of 0.005 M H_2SO_4 at a flow rate of 0.6 mL/min with a run time of 20 min. The product yields were calculated on mole basis as follows:

$$\text{yield\%} = \frac{\text{mol}_{\text{product}}}{\text{mol}_{\text{feedstock}}} \times 100\% \quad (1)$$

The conversion of glucose was calculated as follows:

$$\text{conversion\%} = \left(1 - \frac{\text{mass}_{\text{unconverted}}}{\text{mass}_{\text{feedstock}}}\right) \times 100\% \quad (2)$$

Identification of Tungsten Species. Tungsten species possessed characteristic patterns on ESI-MS spectra. ESI-TOF-MS spectra were recorded on a Bruker MicroTOF-Q system. Both positive and negative modes were employed to monitor the tungsten species in reaction solutions (of various reaction times and temperatures). The samples were injected directly into the chamber at a flow rate of 180 $\mu\text{L}/\text{min}$. Typical instrument parameters were as follows: capillary voltage, 4.5 kV; nebulizer, 1.8 bar; dry gas, 8 L/min at 120 $^\circ\text{C}$; dry temperature, 220 $^\circ\text{C}$; m/z range, 100–2000. Thorough washing by water was conducted between two analyses to avoid interference. The detected liquid solutions were diluted to a concentration of less than 1 mg/mL before analysis.

Isotope-Labeling Tests and NMR Analysis. Two sets of isotope labeling experiments were performed. In the first experiment, unlabeled glucose was mixed with fully labeled glucose (every carbon is labeled, $^{13}\text{C}_6$ -glucose) in equivalent amount to investigate whether the reaction is intermolecular or intramolecular. In the second set of experiments, single-carbon labeled glucose including 1- ^{13}C -glucose, 2- ^{13}C -glucose, and 6- ^{13}C -glucose was used as the reactant to react with ammonia. After reaction, the main product, 2-methyl pyrazine, was analyzed by GC-MS.

Liquid phase ^{13}C NMR was performed on a Bruker ultrashield 400 plus spectrometer. A total of 100 mg of glucose, either in the absence or presence of 100 mg of ammonium metatungstate (AMT), was dissolved in 1 mL of ammonia D_2O solvent. The ammonia D_2O solvent was prepared by constantly purging ammonia gas (pressure 5 bar) into D_2O solution in an autoclave for 30 min. In situ NMR analysis was conducted using $^{13}\text{C}_1$ -glucose as the starting material.

Determination of Homolytic Bond Dissociation Energies. Geometry optimization and single-point energy calculation of the molecules were performed at the B3LYP/6-311++G(d,p) level. All optimized structures were confirmed to be real minima by frequency calculations. For radical fragments, UB3LYP with the same basis set was used. Solvent effects were taken into account implicitly by using the polarizable continuum model (PCM) for water as implemented in Gaussian 09 Revision D.01.⁴⁵

Homolytic bond dissociation energies (BDE) were calculated as follows:

$$\text{BDE} = E(\text{radical fragment A}) + E(\text{radical fragment B}) - E(\text{A} - \text{B}) \quad (3)$$

RESULTS AND DISCUSSION

Tungsten-Assisted Conversion of Glucose in Ammonia Solution. Based on previous reports in catalytic biomass conversion, it is well established that various tungsten-based catalysts show excellent performance in breaking C–C bonds in glucose to form short chain fragments in neutral or acidic environments.^{8,46–50} Therefore, we speculated that these catalysts might also promote the cleavage of glucose in the presence of ammonia to generate C2–C3 species, which could then form the pyrazine ring. Bearing this in mind, we started

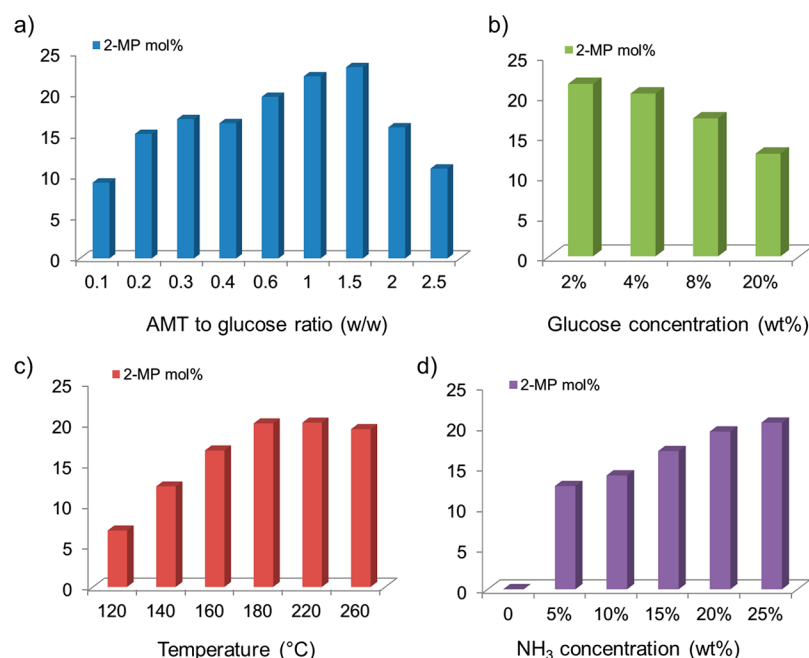


Figure 1. Reaction optimizations of glucose conversion into 2-MP in the presence of AMT catalyst. The effect of (a) AMT to glucose ratios, (b) glucose concentration, (c) temperature, and (d) ammonia concentration. The corresponding variations are made based on the original conditions: 100 mg of glucose, 100 mg of AMT, 5 mL of 25% ammonia solution, 180 °C for 15 min.

the work by converting glucose in concentrated ammonia solution at elevated temperature. In the absence of any catalyst, full glucose conversion was achieved at 180 °C for 15 min, resulting in the formation of a wide range of N-heterocyclic compounds. 4(5)-MI was the major product with 15.3% yield, followed by 2-MP with a yield of 7.8% (optimization data for 2-MP formation without catalysts were provided in Figure S1). Some other pyrazine derivatives such as dimethyl pyrazine and trimethyl pyrazine were detected by GC-MS, although the combined yield of these products was less than 2%. More N-heterocyclic products in trace amounts were detected using the UPLC-ESI-MS technique (see Table S1 and Figure S2). An interesting change of product distribution was observed in the presence of ammonium metatungstate (AMT): the yield of 2-MP was considerably enhanced while negligible changes were found for other products. With an AMT to glucose mass ratio of 0.2 (equivalent to W: glucose mole ratio 0.14), the yield of 2-MP increased from 7.8% to 15.1%, whereas the 4(5)-MI yield remained almost identical (see Figure 1a). With further increase of the AMT to glucose mass ratio, the yields of 2-MP steadily improved and reached 22.1% and 23.2% at the ratio of 1 and 1.5 respectively. The product yield began to decrease when the ratio was higher than 1.5, possibly because excessive catalysts induced side reactions. In an effort to further enhance the yield, coadditives were employed such as metal salts and oxides, but combinational use of AMT and coadditive generally led to a slightly decreased product yield (see Table S2).

The concentration of glucose was gradually increased from 2% to 20% (Figure 1b). Only a slight decrease in 2-MP yield was observed when the glucose concentration changed from 2% to 8%. Even at 20% glucose concentration, the yield of 2-MP reached 12.8%. It shows the feasibility of the reaction system to be applied in relatively concentrated solutions. High temperature had a positive influence on 2-MP yield. The promotional effect of AMT was negligible at 120 °C (data shown in Figures

S1a and 1c), while the yield of 2-MP enhanced accordingly with the temperature elevation from 120 to 180 °C and reached a plateau afterward. A positive correlation between concentration of ammonia and 2-MP yield was observed in the range of 5–25% ammonia (see Figure 1d), but further increasing the NH₃ concentration by purging ammonia gas into the system did not continue to enhance the product yield, indicating that the commercially available 25% ammonia solution was sufficient. Other types of nitrogen sources (NH₄Cl, NH₄COOH, DAP, etc.) were studied (Figure S3), but they performed worse than ammonia solution.

Product Evolution with Reaction Time. The glucose conversion and product profile were monitored with varied reaction times both in the absence or presence of catalysts (see Figures 2 and S8). The consumption of glucose was very rapid. The HPLC data showed that complete glucose conversion was achieved within 5 min, which was in accordance with NMR

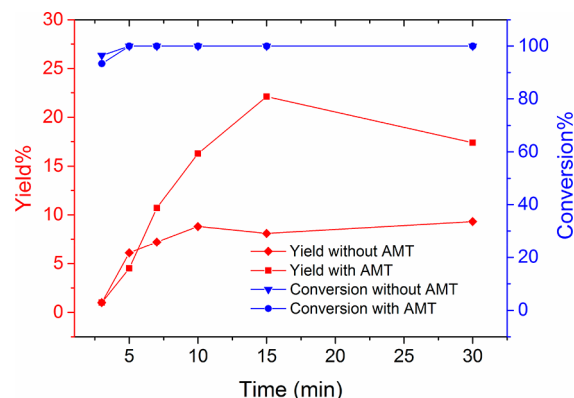


Figure 2. Glucose conversion and 2-MP yield with varied reaction times. Reaction conditions: 100 mg of glucose, 100 mg of AMT or none, 5 mL of 25% ammonia solution, 180 °C for various reaction times.

analysis (Figure S8). Glucose conversion was normally low in neutral water under the temperature we tested (e.g., ca. 35% glucose conversion in water at 180 °C for 3 h),^{51,52} but the basicity provided by ammonia considerably facilitated glucose decomposition. At 3 min, the yield of 2-MP was only 1% either without or with the catalyst, which infers that 2-MP may not be a direct product from glucose. In the absence of catalyst, the product yield slowly increased and stayed at around 9% after a reaction time of 30 min. In contrast, in the presence of AMT, a fast and steady increase in yield was shown after around 6 min and reached the peak value at 15 min, which dropped slightly when prolonging the reaction time to 30 min possibly due to side reactions. The remarkable increase in 2-MP yield at 5 min may indicate the generation of active tungsten species that promoted the product formation (vide infra).

Performance of Other Tungsten Catalysts. Apart from AMT, different types of tungsten-based catalysts were evaluated including ammonium tungstate (AT), tungstic acid (H_2WO_4), silicotungstic acid ($\text{H}_4[\text{W}_{12}\text{SiO}_{40}]$, STA), phosphotungstic acid ($\text{H}_3\text{PW}_{12}\text{O}_{40}$, PTA), sodium tungstate (Na_2WO_4), lithium tungstate (Li_2WO_4), magnesium tungstate (MgWO_4), calcium tungstate (CaWO_4), and WO_3 . The catalysts were compared under identical reaction conditions, at a catalyst to glucose mass ratio of 0.2 (see Figure 3). WO_3 , AT, and STA exhibited similar

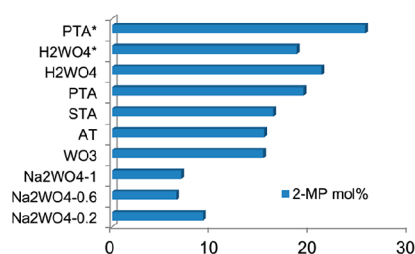


Figure 3. 2-MP yields with different types of tungsten-based catalysts. Reaction conditions: 100 mg of glucose, 20 mg of catalyst, 5 mL of 25% ammonia solution, 180 °C for 15 min. * means 100 mg catalyst was used.

performances as compared to AMT, leading to 2-MP yields of 15.3%, 15.4%, and 16.3%, respectively, whereas the yields were slightly higher in the presence of PTA and H_2WO_4 , reaching 19.4% and 21.2%, respectively. Promotional effects were also observed over these compounds at a tungsten catalyst to glucose mass ratio of 1. Among all tungsten-based catalysts tested, surprisingly, $\text{M}_x(\text{WO}_4)_y$ exhibited no promotional effect or even a negative effect in product formation. For instance, with Na_2WO_4 to glucose ratio varying from 0.2 to 1, 2-MP yields were 9.2%, 6.5%, and 7%, respectively, even lower than the yield achieved in the blank test. Other tungstic acid salts such as Li_2WO_4 , MgWO_4 , and CaWO_4 led to low 2-MP yields around 8% as well (Table S3, entries 6–8). Interestingly, H_2WO_4 , which has a very similar starting structure with Na_2WO_4 , is an excellent catalyst. To understand the cation effect, control experiments were undertaken by using NaCl and NaNO_3 (Table S3, entries 1 and 2), which shows that the sodium salts alone do not have negative effects on 2-MP formation. Next, a mixture of NaCl and H_2WO_4 (catalyst to glucose ratio of 0.2) was added and 2-MP yield dropped for about 40% (from 21.2% to 13.0%, Table S3, entry 3). Thus, it is likely that WO_4^{2-} is a precursor for real active species, but the existence of Na^+ hinders the formation of that (these) species. Interestingly, the inhibitory effect of Na^+ was negligible when

using a mixture of NaCl and WO_3 (Table S3, entry 4 and 5), in which the 2-MP yield reached 21.2%.

Monitoring Active Tungsten Species. The screening results of tungsten catalysts strongly suggest that neither monotungsten species such as WO_4^{2-} nor heterogeneous WO_3 particles were the real catalyst. ESI-MS technique was therefore employed to reveal the plausible species responsible for pyrazine formation in the system. First, we examined tungsten species in neutral water and ammonia solution using AMT as the precatalyst (see Figure S4). In neutral water, large tungsten clusters such as $[\text{H}_4\text{W}_{12}\text{O}_{40}]^{4-}$ and $[\text{H}_3\text{W}_{12}\text{O}_{39}]^{3-}$ were the dominant species. In the basic ammonia solution, decomposition of the large clusters occurred and small species such as $[\text{HWO}_4]^-$ and $[\text{HW}_2\text{O}_7]^-$ became the major fraction. Upon heating, small clusters disappeared and $[\text{HWO}_4]^-$ was dominant. Hence, basic conditions led to the dissociation of the large tungsten clusters. Next, various active tungsten catalysts were analyzed by ESI-MS, and the spectra were compared with the inactive Na_2WO_4 precatalyst (Figure 4a). Although $[\text{HWO}_4]^-$ was predominant in all of the samples, the formation of a group of small tungsten clusters (from m/z ca. 400 to 1000) has been noticed for all of the active catalyst species such as AMT and H_2WO_4 , which was totally absent in the spectrum of Na_2WO_4 . The small clusters range from W_2 to W_6 species including $[\text{HW}_2\text{O}_7]^-$, $[\text{H}_3\text{W}_3\text{O}_{10}]^-$, $[\text{W}_4\text{O}_{13}]^{2-}$, $[\text{W}_5\text{O}_{16}]^{2-}$, and $[\text{W}_6\text{O}_{19}]^{2-}$. These small clusters, which were only present in the ammonia solutions of active precatalysts, were possibly responsible for the enhanced 2-MP yields.

We further introduced glucose into the system containing AMT precatalyst and scrutinized the evolution of tungsten species with time under reaction conditions (Figure 4b,c). At 0 min, apart from the peaks of small tungsten species such as $[\text{HWO}_4]^-$, the signals of large tungsten clusters such as $[\text{H}_4\text{W}_{12}\text{O}_{40}]^{4-}$, $[\text{H}_3\text{W}_{12}\text{O}_{40}]^{3-}$, and $[\text{H}_4\text{W}_{12}\text{O}_{39}]^{2-}$ were observable. More importantly, glucose–tungsten complexes were observed such as $[\text{C}_6\text{H}_{12}\text{O}_6\text{HWO}_3]^-$, $[\text{2C}_6\text{H}_{10}\text{O}_6\text{HWO}_2]^-$, $[\text{C}_6\text{H}_{12}\text{O}_6\text{HW}_2\text{O}_6]^-$, and $[\text{2C}_6\text{H}_{10}\text{O}_6\text{HW}_2\text{O}_5]^-$, showing the close interaction between tungsten and glucose. After heating for 3 min, the signals of W_{12} clusters disappeared, and thus these large species were unstable under reaction conditions and could not be the active components. Meanwhile, the peaks assigned to the glucose–tungsten complexes changed the shape with increased number of peaks (see Figure 4c), and the peak centers shifted to m/z (M-1). For example, the peak centers shifted from m/z 411 to 410, from 573 to 572, etc. After heating for 5 min, the number of the peaks was reduced, with the center of the peaks unambiguously located at the position of (M-1). The phenomenon is a strong indication for the formation of an amino-sugar at 3 min, which has the molecular weight one less than glucose because of the replacement of a $-\text{OH}$ group with an $-\text{NH}_2$ group.

The formation of the amino-sugar has been confirmed by NMR analysis (see Figure S5). The NMR spectrum of the initial solution shows that the system was relatively pure with six dominant peaks at 84.7, 76.5, 76.1, 73.9, 69.4, and 60.4 ppm. The signals of glucose were very weak, consistent with the product evolution profile (see Figure 2) showing that the majority of glucose was converted at 3 min. The peaks at 95.6 and 91.7 ppm were assigned to C1 of glucose α - and β -anomers, respectively. Hence, the $-\text{NH}_2$ group was attached on C1 in the product, which has been identified to be β -D-glucopyranosylamine according to the literature.⁵³ Without a catalyst, the formation of the amino sugar in ammonia solution

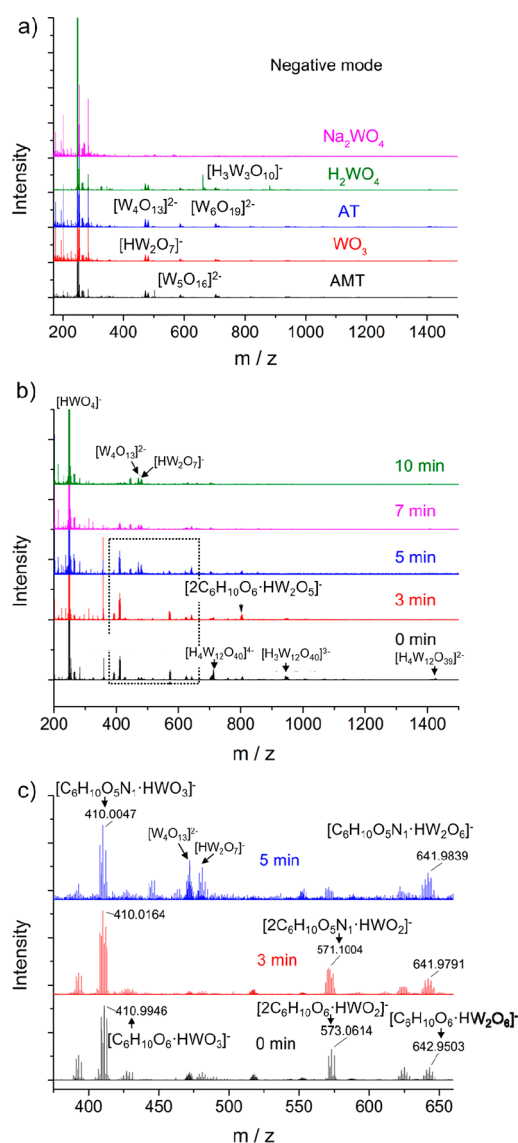


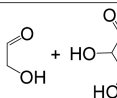
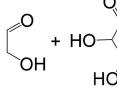
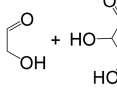
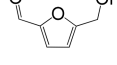
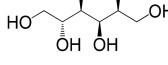
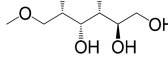
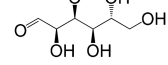
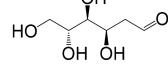
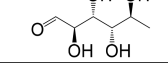
Figure 4. (a) ESI signals (negative mode) of different types of tungsten-based catalysts and (b) ESI signals (negative mode) of reaction solutions with various reaction times. Reaction conditions: 100 mg of glucose, 100 mg of AMT, 5 mL of ammonia solution, 180 °C for various times. The reaction solutions were 100-fold diluted for ESI analysis, and (c) the enlarged figure of the rectangular area in panel b.

required several days at the same temperature.⁵⁴ For comparison, the ESI spectra of glucose with AMT and Na_2WO_4 under identical conditions were examined (see Figure S6), and β -D-glucopyranosylamine was selectively formed from glucose only in the presence of AMT. Therefore, β -D-glucopyranosylamine, which is generally more reactive than glucose and formed at a very early stage, is plausibly a key intermediate for the selective formation of 2-MP. With reaction time increased to 7 and 10 min (see Figure 4b), the tungsten–amino sugar complexes almost disappeared indicating the decomposition of glucosylamine as the reaction progressed. Concurrently, a drastic increase in peak intensity at m/z 472.0 and 481.0 at 5 min was observed, which were ascribed to be $[\text{HW}_2\text{O}_7]^-$ and $[\text{W}_4\text{O}_{13}]^{2-}$ species, respectively. These tungsten clusters are likely to be the main catalytically active species because (1) they were absent when Na_2WO_4 was used,

(2) glucose– W_2 and glucosylamine– W_2 complexes were observed, and (3) the 2-MP yield started to enhance significantly from 5 min (see the figure).

Model Compound Experiments. We propose that β -D-glucopyranosylamine decomposed into smaller fragments (C_2 and C_3 species) for further formation of 2-MP. As such, several C_2 and C_3 compounds (the basic units to form 2-MP ring) were used as the starting material to simulate fragments from β -D-glucopyranosylamine. Glycolaldehyde dimer and glyceraldehyde were selected because they are commercially available and relatively stable. Equal mole amounts of glycolaldehyde dimer and glyceraldehyde were mixed and reacted, and the 2-MP yields were 8.6% without a catalyst and about 15% in the presence of AMT (see Table 1, entries 1–3). It suggests that

Table 1. 2-MP Yields Starting from Different Model Compounds^a

Entry	Substrate(s)	Catalyst to substrate ratio	2-MP mol%
1		None	8.6
2		0.2	14.4
3		1	15.1
4		1	4.9
5		1	0.0
6		1	0.1
7		1	0.0
8		1	0.8
9		1	0.2

^aReaction conditions: 100 mg of substrate, certain ratio of AMT catalyst (w/w), 5 mL of 25% ammonia solution, 180 °C for 15 min.

the tungsten catalyst also promoted the ring formation of the small fragments, possibly because tungsten can coordinate with the C_2 and C_3 species to stabilize the highly active fragments. Other model compounds were employed to gather additional information on the reaction pathway. For example, starting from 5-HMF, the 2-MP yield was very low, ruling out the pathway of 2-MP formation via furan intermediates. When sorbitol was used as a substrate, the yield of 2-MP was negligible. This emphasizes the crucial role of the aldehyde group on C1 position for 2-MP generation. Next, specific site blocked glucose analogs including 1-O-methyl glucose, 3-O-methyl glucose, 2-deoxy-D-glucose, and L-rhamnose were

employed, and all of them resulted in negligible yields of 2-MP (see Table 1). As a result, the OH groups in glucose are important for the formation of 2-MP and missing any single one blocks the formation route of 2-MP.

Reaction Pathways: Isotope Labeling Tests. In the literature, there are two main reaction pathways proposed for glucose conversion to N-heterocyclic compounds in ammonia solution.²⁸ The first assumption suggests the initial formation of glucosylamine and then aminodeoxy sugars, which undergo intermolecular self-condensation and dehydration to generate the pyrazine ring. Thermal decomposition of the long side chain led to 2-methyl pyrazine and other products. The second assumption is the fragmentation mechanism, which involves the amination of glucose, followed by different pathways to form C₂ and C₃ species which then condensate and dehydrate to yield 2-MP.

To shed light on the reaction pathway in our system, ¹³C-labeled glucose substrates were used, and the product was analyzed by GC-MS. As a control experiment, the GC spectrum of the reaction solution from unlabeled glucose was examined, which exhibited relatively simple patterns (see Figure 5a). The

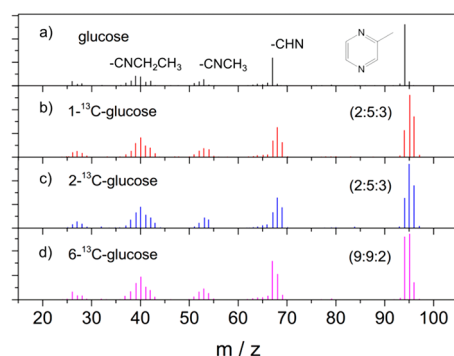


Figure 5. ¹³C-labeling isotope tests of (a) unlabeled glucose, (b) 1-¹³C-glucose, (c) 2-¹³C-glucose, and (d) 6-¹³C-glucose. Reaction conditions: 100 mg of substrate, 100 mg of AMT, 5 mL of ammonia solution, 180 °C for 15 min.

molecule ion peak of 2-MP was at m/z 94 as a single peak, and the isotope peak at m/z 95 was negligible. When using 1-¹³C-glucose, 2-¹³C-glucose, and 6-¹³C-glucose (Figure 5b–d), the molecule ion peaks diverges into three peaks at m/z 94, 95, and 96. The presence of these three peaks ruled out the possibility of the first reaction pathway. This is because if intermolecular self-condensation happened, starting from 1-¹³C-glucose or 2-¹³C-glucose, there would be only two peaks as the molecule ion peaks at m/z 94 and 96, whereas starting from 6-¹³C-glucose, the molecule ion peak should be a single peak at m/z 94. The fragmentation mechanism is therefore the dominant reaction pathway in the current study. When using a mixture of unlabeled glucose and fully ¹³C-labeled glucose (1:1; see Figure S7), four major peaks (m/z 94, 96, 97, and 99) were identified as the molecule ion peaks, which was exactly expected if the reaction follows a fragmentation pathway.

Interestingly, the structure of 2-MP is asymmetric requiring the combination of a C₂ with a C₃ species. The primary fragmentation of the C₆ molecule could produce C₂ + C₄ or C₃ + C₃ species, and secondary fragmentation of the C₄ species into C₃ and C₁ or of C₃ species into C₂ and C₁ may also occur. The presence of the peak at m/z 96 when using 1-¹³C-glucose and 2-¹³C-glucose, meaning two ¹³C atoms are present in the

product, either suggests the primary fragmentation pathway to involve both the C₂ + C₄ and C₃ + C₃ cleavage patterns or an equilibrium between glyceraldehyde and dihydroxyacetone and their imine derivatives. Based on DFT calculations for the homolytic bond dissociation energies, the cleavage of glucose or its imine into C₄ + C₂ is plausible. Furthermore, the obtained species can undergo further cleavage into either two C₂ species or one C₃ and one C₁ species. Besides, another potential way to form C₃ species is that the glucose imine is isomerized to the fructose derivative and then is cleaved in a subsequent retro-aldol reaction. Although fructose was never observed during the reaction, it is possibly because its consumption was faster than its accumulation. To prove this, experiments were carried out using fructose as a substrate in comparison with glucose. Indeed, the reaction rate constant of the reaction using fructose (0.013 s⁻¹) was significantly larger than that of glucose (0.0092 s⁻¹).

A plausible reaction pathway to form 2-MP from glucose has been proposed based on the above analysis (see Figure 6). First, glucose is rapidly converted into β-D-glucopyranosylamine prompted by tungsten catalyst. The following pathway diverges into three different directions. First, the glucose derivative can undergo a retro-aldol reaction to form a C₂ and a C₄ species followed by further cleavage into either two C₂ species or one C₃ and one C₁ species. On the other side, a Lobry de Bruyn–Alberda–van Ekenstein transformation yields the fructose derivative that is cleaved into two C₃ species. Probably, they are in equilibrium to each other and the glyceraldehyde derivative is proposed to be further converted into a C₂ and a C₁ species. Finally, a condensation and a dehydration step yield the product 2-MP.

Scope of Renewable Sugars. The reaction system is applicable to a variety of monosaccharides (see Figure 7). Xylose, a key monomer of hemicellulose, afforded a slightly higher 2-MP yield of 23.3% than glucose. This is not unexpected, since xylose as a pentose could more conveniently generate C₂ and C₃ species via fragmentation. Glucosamine, derived from chitosan, generated 2-MP in 18.3% yield, similar to the product yield of fructose. Starting from NAG (chitin monomer), the 2-MP yield dropped considerably to around 7.2%, which was less than half of the yields from other monosaccharides, suggesting the necessity of hydrolysis of the acetamido group into an amine group for product formation. Disaccharides were also used as the starting material. Cellobiose, maltose, and sucrose afforded yields of 10.3%, 10.5%, and 0.5%, respectively. It indicates that the nature of the glycosidic bond has a profound influence. Cellobiose and maltose with either β (1 → 4) or α (1 → 4) glycosidic bonds led to comparable 2-MP yields of around 10%, whereas sucrose with a (1 → 2) glycosidic bond resulted in only 0.5% product yield. Based on the reaction pathway, this could be rationalized as the blockage effect of the (1 → 2) linkage to both the aldehyde group in the glucose unit and the ketone group in the fructose unit, which inhibits the substrate transformation to the glucosylamine intermediate. The inadequacy of the reaction system for the cleavage of glycosidic linkage was further revealed when polysaccharides were employed. The 2-MP yields were 0.4% and 2.1% from cellulose and ball-milled cellulose, while no 2-MP product was identified using inulin and pectin. As a result, the reaction system is highly effective for monosaccharides, applicable to some extent for disaccharides but not efficient for polysaccharides.

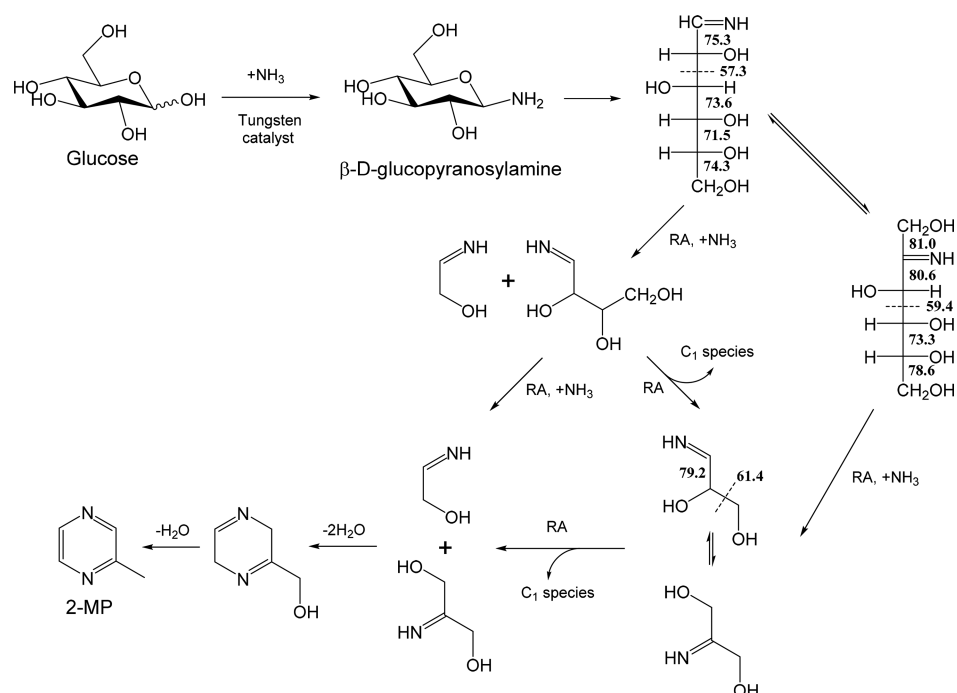


Figure 6. Proposed reaction pathway of glucose conversion into 2-MP product, homolytic C–C bond dissociation energies for three of the molecules are indicated (kcal/mol), RA indicates retro-aldol reaction.

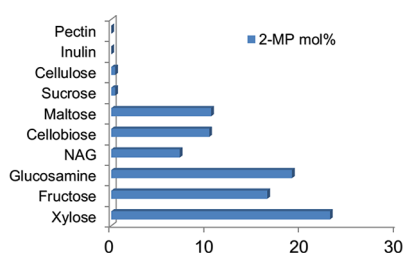


Figure 7. 2-MP yields starting from different sugars and polysaccharides. Reaction conditions: 100 mg of substrate, 100 mg of AMT catalyst, 5 mL of 25% ammonia solution, 180 °C for 15 min.

CONCLUSIONS

In this paper, a tungsten-based catalytic system has been developed to efficiently convert monosaccharides into N-heterocyclic products in aqueous ammonia. Under optimal conditions, 2-MP formed rapidly (within 15 min) with the highest yield of 25.6% from glucose in a single step, while 15% 4(S)-MI was simultaneously obtained. We identified β -D-glucopyranosylamine as an important intermediate and the fragmentation mechanism to be the major reaction pathway. The tungsten catalyst promotes both the chain cleavage and cyclization steps, with W_2 – W_4 species as plausible active species for the transformation. The catalytic system is applicable to other monosaccharides and some disaccharides. The work points out new possibilities on the sustainable production of N-heterocyclic compounds from biomass resources through simple, catalytic routes.

ASSOCIATED CONTENT

Supporting Information

The Supporting Information is available free of charge on the ACS Publications website at DOI: 10.1021/acssuschemeng.7b03048.

Reaction optimization of glucose in ammonia solution without catalyst; other minor products as quantified by GC-FID; UPLC-MS and ESI-MS spectra of the reaction solution; 2-MP yields with coadditives of AMT and different metal salts; 2-MP yields with different ammonia sources; 2-MP yields with different tungsten-based catalysts; ^{13}C NMR of the reaction solution in ammonia D_2O ; isotope-labeling test. (PDF)

AUTHOR INFORMATION

Corresponding Author

*E-mail: ning.yan@nus.edu.sg.

ORCID

Ning Yan: 0000-0002-1877-9206

Notes

The authors declare no competing financial interest.

ACKNOWLEDGMENTS

The authors gratefully acknowledge the Young Investigator Award from National University of Singapore (WBS: R-279-000-464-133), MOE Tier-2 grant (WBS: R-279-000-462-112), and MOE Tier-1 grant (WBS: R-279-000-438-112).

REFERENCES

- (1) Sanderson, K. Lignocellulose: a chewy problem. *Nature* **2011**, 474 (7352), S12–S14.
- (2) Zhu, Y.; Romain, C.; Williams, C. K. Sustainable polymers from renewable resources. *Nature* **2016**, 540 (7633), 354–362.
- (3) Luterbacher, J. S.; Rand, J. M.; Alonso, D. M.; Han, J.; Youngquist, J. T.; Maravelias, C. T.; Pfleger, B. F.; Dumesic, J. A. Nonenzymatic sugar production from biomass using biomass-derived γ -valerolactone. *Science* **2014**, 343 (6168), 277–280.
- (4) Ma, R.; Guo, M.; Lin, K.-t.; Hebert, V. R.; Zhang, J.; Wolcott, M. P.; Quintero, M.; Ramasamy, K. K.; Chen, X.; Zhang, X. Peracetic Acid Depolymerization of Biorefinery Lignin for Production of Selective

Monomeric Phenolic Compounds. *Chem. - Eur. J.* **2016**, *22* (31), 10884–10891.

(5) Alvarez-Vasco, C.; Ma, R.; Quintero, M.; Guo, M.; Geleynse, S.; Ramasamy, K. K.; Wolcott, M.; Zhang, X. Unique low-molecular-weight lignin with high purity extracted from wood by deep eutectic solvents (DES): a source of lignin for valorization. *Green Chem.* **2016**, *18* (19), 5133–5141.

(6) Kennema, M.; de Castro, I. B. D.; Meemken, F.; Rinaldi, R. Liquid-Phase H-Transfer from 2-Propanol to Phenol on Raney Ni: Surface Processes and Inhibition. *ACS Catal.* **2017**, *7* (4), 2437–2445.

(7) Calvaruso, G.; Clough, M. T.; Rinaldi, R. Biphasic extraction of mechanocatalytically-depolymerized lignin from water-soluble wood and its catalytic downstream processing. *Green Chem.* **2017**, *19* (12), 2803–2811.

(8) Wang, A.; Zhang, T. One-Pot Conversion of Cellulose to Ethylene Glycol with Multifunctional Tungsten-Based Catalysts. *Acc. Chem. Res.* **2013**, *46* (7), 1377–1386.

(9) Kobayashi, H.; Kaiki, H.; Shrotri, A.; Techikawara, K.; Fukuoka, A. Hydrolysis of woody biomass by a biomass-derived reusable heterogeneous catalyst. *Chem. Sci.* **2016**, *7* (1), 692–696.

(10) Fan, J.; De Bruyn, M.; Budarin, V. L.; Gronnow, M. J.; Shuttleworth, P. S.; Breeden, S.; Macquarrie, D. J.; Clark, J. H. Direct Microwave-Assisted Hydrothermal Depolymerization of Cellulose. *J. Am. Chem. Soc.* **2013**, *135* (32), 11728–11731.

(11) Zhang, J.; Asakura, H.; van Rijn, J.; Yang, J.; Duchesne, P.; Zhang, B.; Chen, X.; Zhang, P.; Saeys, M.; Yan, N. Highly Efficient, NiAu-catalyzed Hydrogenolysis of Lignin into Phenolic Chemicals. *Green Chem.* **2014**, *16*, 2432–2437.

(12) Zhang, J.; Teo, J.; Chen, X.; Asakura, H.; Tanaka, T.; Teramura, K.; Yan, N. A Series of NiM (M = Ru, Rh, and Pd) Bimetallic Catalysts for Effective Lignin Hydrogenolysis in Water. *ACS Catal.* **2014**, *4*, 1574–1583.

(13) Besson, M.; Gallezot, P.; Pinel, C. Conversion of Biomass into Chemicals over Metal Catalysts. *Chem. Rev.* **2014**, *114* (3), 1827–1870.

(14) Upton, B. M.; Kasko, A. M. Strategies for the Conversion of Lignin to High-Value Polymeric Materials: Review and Perspective. *Chem. Rev.* **2016**, *116* (4), 2275–2306.

(15) Siankevich, S.; Savoglidis, G.; Fei, Z.; Laurenczy, G.; Alexander, D. T. L.; Yan, N.; Dyson, P. J. A novel platinum nanocatalyst for the oxidation of 5-Hydroxymethylfurfural into 2,5-Furandicarboxylic acid under mild conditions. *J. Catal.* **2014**, *315* (0), 67–74.

(16) Siankevich, S.; Fei, Z.; Scopelliti, R.; Jessop, P. G.; Zhang, J.; Yan, N.; Dyson, P. J. Direct Conversion of Mono- and Polysaccharides into 5-Hydroxymethylfurfural Using Ionic-Liquid Mixtures. *ChemSusChem* **2016**, *9* (16), 2089–2096.

(17) Zhang, J.; Zhao, C. Development of a Bimetallic Pd-Ni/HZSM-5 Catalyst for the Tandem Limonene Dehydrogenation and Fatty Acid Deoxygenation to Alkanes and Arenes for Use as Biojet Fuel. *ACS Catal.* **2016**, *6* (7), 4512–4525.

(18) Wu, L.; Li, L.; Li, B.; Zhao, C. Selective conversion of coconut oil to fatty alcohols in methanol over a hydrothermally prepared Cu/SiO₂ catalyst without extraneous hydrogen. *Chem. Commun.* **2017**, *53* (45), 6152–6155.

(19) Yoon, J. S.; Lee, T.; Choi, J.-W.; Suh, D. J.; Lee, K.; Ha, J.-M.; Choi, J. Layered MWW zeolite-supported Rh catalysts for the hydrodeoxygenation of lignin model compounds. *Catal. Today* **2017**, *293*, 142–150.

(20) Tang, C.; Shen, T.; Jiao, N. Introduction. In *Nitrogenation Strategy for the Synthesis of N-containing Compounds*; Jiao, N., Ed.; Springer Singapore: Singapore, 2017; pp 1–8.

(21) Yan, N.; Chen, X. Sustainability: Don't waste seafood waste. *Nature* **2015**, *524* (7564), 155–157.

(22) Brun, N.; Hesemann, P.; Esposito, D. Expanding the biomass derived chemical space. *Chem. Sci.* **2017**, *8*, 4724.

(23) Maiti, S.; Biswas, S.; Jana, U. Iron(III)-Catalyzed Four-Component Coupling Reaction of 1,3-Dicarbonyl Compounds, Amines, Aldehydes, and Nitroalkanes: A Simple and Direct Synthesis of Functionalized Pyrroles. *J. Org. Chem.* **2010**, *75* (5), 1674–1683.

(24) Rizk, T.; Bilodeau, E. J. F.; Beauchemin, A. M. Synthesis of Pyridines and Pyrazines Using an Intramolecular Hydroamination-Based Reaction Sequence. *Angew. Chem., Int. Ed.* **2009**, *48* (44), 8325–8327.

(25) Gnanaprakasam, B.; Balaraman, E.; Ben-David, Y.; Milstein, D. Synthesis of Peptides and Pyrazines from β -Amino Alcohols through Extrusion of H₂ Catalyzed by Ruthenium Pincer Complexes: Ligand-Controlled Selectivity. *Angew. Chem.* **2011**, *123* (51), 12448–12452.

(26) Venugopal, A.; Sarkari, R.; Anjaneyulu, C.; Krishna, V.; Kumar, M. K.; Narender, N.; Padmasri, A. H. Influence of acid-base sites on ZnO–ZnCr 2 O 4 catalyst during dehydrocyclization of aqueous glycerol and ethylenediamine for the synthesis of 2-methylpyrazine: Kinetic and mechanism studies. *Appl. Catal., A* **2014**, *469*, 398–409.

(27) Milić, B. L.; Piletić, M. V. The mechanism of pyrrole, pyrazine and pyridine formation in non-enzymic browning reaction. *Food Chem.* **1984**, *13* (3), 165–180.

(28) Kort, M. J. Reactions of Free Sugars with Aqueous Ammonia**The author thanks Professor D.A. Sutton for suggesting that this subject be reviewed. *Adv. Carbohydr. Chem. Biochem.* **1970**, *25*, 311–349.

(29) Lichtenthaler, F. W. Unsaturated O- and N-Heterocycles from Carbohydrate Feedstocks. *Acc. Chem. Res.* **2002**, *35* (9), 728–737.

(30) Shibamoto, T.; Bernhard, R. A. Investigation of pyrazine formation pathways in sugar-ammonia model systems. *J. Agric. Food Chem.* **1977**, *25* (3), 609–614.

(31) Gao, X.; Chen, X.; Zhang, J.; Guo, W.; Jin, F.; Yan, N. Transformation of Chitin and Waste Shrimp Shells into Acetic Acid and Pyrrole. *ACS Sustainable Chem. Eng.* **2016**, *4* (7), 3912–3920.

(32) Song, L.; Zheng, M.; Pang, J.; Sebastian, J.; Wang, W.; Qu, M.; Zhao, J.; Wang, X.; Zhang, T. One-pot synthesis of 2-hydroxymethyl-5-methylpyrazine from renewable 1,3-dihydroxyacetone. *Green Chem.* **2017**, *19* (15), 3515–3519.

(33) Chen, X.; Yang, H.; Yan, N. Shell Biorefinery: Dream or Reality? *Chem. - Eur. J.* **2016**, *22* (38), 13402–13421.

(34) Pierson, Y.; Chen, X.; Bobbink, F. D.; Zhang, J.; Yan, N. Acid-Catalyzed Chitin Liquefaction in Ethylene Glycol. *ACS Sustainable Chem. Eng.* **2014**, *2* (8), 2081–2089.

(35) Bobbink, F. D.; Zhang, J.; Pierson, Y.; Chen, X.; Yan, N. Conversion of chitin derived N-acetyl-d-glucosamine (NAG) into polyols over transition metal catalysts and hydrogen in water. *Green Chem.* **2015**, *17* (2), 1024–1031.

(36) Chen, X.; Chew, S. L.; Kerton, F. M.; Yan, N. Direct conversion of chitin into a N-containing furan derivative. *Green Chem.* **2014**, *16* (4), 2204–2212.

(37) Chen, X.; Liu, Y.; Kerton, F. M.; Yan, N. Conversion of chitin and N-acetyl-d-glucosamine into a N-containing furan derivative in ionic liquids. *RSC Adv.* **2015**, *5* (26), 20073–20080.

(38) Chen, X.; Gao, Y.; Wang, L.; Chen, H.; Yan, N. Effect of Treatment Methods on Chitin Structure and Its Transformation into Nitrogen-Containing Chemicals. *ChemPlusChem* **2015**, *80* (10), 1565–1572.

(39) Drover, M. W.; Omari, K. W.; Murphy, J. N.; Kerton, F. M. Formation of a renewable amide, 3-acetamido-5-acetylfuran, via direct conversion of N-acetyl-d-glucosamine. *RSC Adv.* **2012**, *2* (11), 4642–4644.

(40) Wang, Y.; Pedersen, C. M.; Deng, T.; Qiao, Y.; Hou, X. Direct conversion of chitin biomass to 5-hydroxymethylfurfural in concentrated ZnCl₂ aqueous solution. *Bioresour. Technol.* **2013**, *143* (0), 384–390.

(41) Osada, M.; Kikuta, K.; Yoshida, K.; Totani, K.; Ogata, M.; Usui, T. Non-catalytic synthesis of Chromogen I and III from N-acetyl-d-glucosamine in high-temperature water. *Green Chem.* **2013**, *15* (10), 2960–2966.

(42) Szabolcs, Á.; Molnár, M.; Dibó, G.; Mika, L. T. Microwave-assisted conversion of carbohydrates to levulinic acid: an essential step in biomass conversion. *Green Chem.* **2013**, *15* (2), 439–445.

(43) Ohmi, Y.; Nishimura, S.; Ebitani, K. Synthesis of α -Amino Acids from Glucosamine-HCl and its Derivatives by Aerobic Oxidation in

Water Catalyzed by Au Nanoparticles on Basic Supports. *ChemSusChem* **2013**, *6* (12), 2259–2262.

(44) Chen, X.; Yang, H.; Zhong, Z.; Yan, N. Base-catalysed, one-step mechanochemical conversion of chitin and shrimp shells into low molecular weight chitosan. *Green Chem.* **2017**, *19*, 2783.

(45) Frisch, M.; et al. *Gaussian 09*, revision D.01; Gaussian, Inc.: Wallingford, CT, 2009.

(46) Ji, N.; Zhang, T.; Zheng, M.; Wang, A.; Wang, H.; Wang, X.; Chen, J. G. Direct Catalytic Conversion of Cellulose into Ethylene Glycol Using Nickel-Promoted Tungsten Carbide Catalysts. *Angew. Chem.* **2008**, *120* (44), 8638–8641.

(47) Zhang, J.; Liu, X.; Sun, M.; Ma, X.; Han, Y. Direct Conversion of Cellulose to Glycolic Acid with a Phosphomolybdic Acid Catalyst in a Water Medium. *ACS Catal.* **2012**, *2* (8), 1698–1702.

(48) Liu, Y.; Luo, C.; Liu, H. Tungsten trioxide promoted selective conversion of cellulose into propylene glycol and ethylene glycol on a ruthenium catalyst. *Angew. Chem.* **2012**, *124* (13), 3303–3307.

(49) Zhao, G.; Zheng, M.; Zhang, J.; Wang, A.; Zhang, T. Catalytic Conversion of Concentrated Glucose to Ethylene Glycol with Semicontinuous Reaction System. *Ind. Eng. Chem. Res.* **2013**, *52* (28), 9566–9572.

(50) Yunarti, R. T.; Gu, S.; Choi, J.-W.; Jae, J.; Suh, D. J.; Ha, J.-M. Oxidative Coupling of Methane Using Mg/Ti-Doped SiO₂-Supported Na₂WO₄/Mn Catalysts. *ACS Sustainable Chem. Eng.* **2017**, *5* (5), 3667–3674.

(51) Jing, Q.; LÜ, X. Kinetics of Non-catalyzed Decomposition of Glucose in High-temperature Liquid Water. *Chin. J. Chem. Eng.* **2008**, *16* (6), 890–894.

(52) Knežević, D.; van Swaaij, W. P. M.; Kersten, S. R. A. Hydrothermal Conversion of Biomass: I, Glucose Conversion in Hot Compressed Water. *Ind. Eng. Chem. Res.* **2009**, *48* (10), 4731–4743.

(53) Muhizi, T.; Coma, V.; Grelier, S. Synthesis and evaluation of N-alkyl-β-d-glucosylamines on the growth of two wood fungi, *Coriolus versicolor* and *Poria placenta*. *Carbohydr. Res.* **2008**, *343* (14), 2369–2375.

(54) Tang, P.-P.; Cai, J.-B.; Gao, Y.; Su, Q.-D. Preparation and Evaluation of a Molecular Recognition Bionic Solid Phase Extraction Column for Separation of Glucosides. *J. Chin. Chem. Soc.* **2010**, *57* (6), 1248–1256.